Chemical Science

Accepted Manuscript

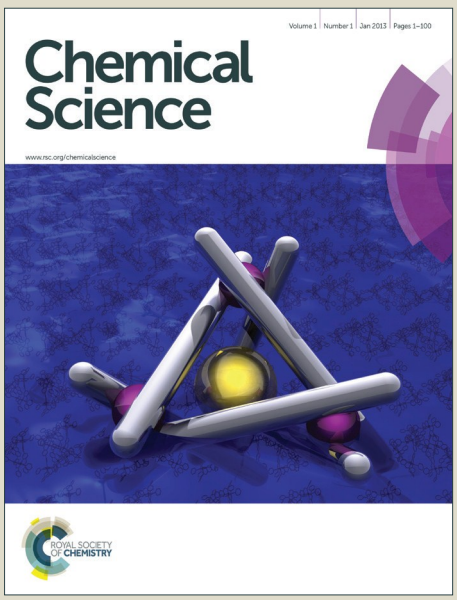

ROYAL SOCIETY OF CHEMISTRY

www.rsc.org/chemicalscience

Journal Name

Chemical Science

Dynamic Article Links ►

Cite this: DOI: 10.1039/c0xx00000x

www.rsc.org/xxxxxx

ARTICLE TYPE

ATP-triggered biomimetic deformations of bioinspired receptor-containing polymer assemblies

Qiang Yan, and Yue Zhao*

Received (in XXX, XXX) Xth XXXXXXXXX 20XX, Accepted Xth XXXXXXXXX 20XX

DOI: 10.1039/b000000x

Designing synthetic polymer assemblies that can sense a biological signal to mimic cell activities is elusive. We develop a class of block copolymer containing bioinspired host units as supramolecular catcher for high-selective capture of adenosine-5'-triphosphate (ATP). Driven by ATP, these block copolymers undergo a stepwise self-assembly and exhibit cascading deformation into high-ordered nanostructures via the specific recognition effect between ATP and the receptor. Modulating the ATP concentrations, one can precisely control biomimetic evolution of these assemblies in diverse dimensionalities and geometries, like certain organellar deformations. Moreover, the ATP/polymer hybrid aggregates can be reversibly disassembled in response to phosphatase. This special ability of the artificial assemblies to sense intracellular bioactivators can offer new insight on bio-responsive nanomaterials for cellular applications.

Introduction

Responding to specific intracellular biological signals is one of the most inherent features of living organism, which is crucial for maintaining cell activities, especially the biological deformable motions.[1] Controlled shape transformation tuned by endogenous molecules is ubiquitous in biological systems.[2] Although they offer us many references,[3] considering their componential multiplicity and self-organized complexity, it is greatly difficult to simulate these deformations via artificial molecular building blocks.[4] Seeking new methodology to build molecular assemblies that can sense biomolecules to drive shape transformation is conducive to bridging self-assembly chemistry and biomimicry.

In this respect, stimuli-responsive polymeric assemblies have sparked considerable interest since they can respond to physical or chemical changes (e.g. pH, temperature, redox, gas, and light), and trigger a self-assembled shape transformation.[5] To date, the known polymer stimuli-deformation involves three fundamental principles: (i) the cleavage/linkage of chemical bonds, (ii) the configuration conversion of groups, and (iii) the phase transition of polymer chains.[6] In contrast, the deformation of biological assemblies is usually mediated by a ligand-receptor effect, that is, bioactivator (acting as the ligand) can be captured by specific bio-receptor for tuning their morphologies. However, the majority of synthetic macromolecules have the limitation on binding such bioactivators.[7] It is intelligible since biological molecules are too intricate to selective recognize.[8] Hence designing novel polymer with bioinspired receptors capable of responding to cellular signal remains a tremendous challenge.[9]

ATP, as cellular energy currency, is a central metabolite and critical biological signaling molecule, playing an irreplaceable role in many cell activities. Some nascent studies made use of natural aptamers or chaperone proteins to prepare ATP-sensitive nanocarriers.[10] In these systems, ATP molecules can manipulate the disassembly of these nanocarriers. Despite of the progress on this frontier, synthetic polymers that can feedback ATP biosignal have not been developed so far. Thereby, exploiting ATP as an endogenous stimulus to subtly modulate the dynamic behaviors of polymer assemblies holds promise for biomimicry.

Natural ATP carrier protein has a funnel-like structure (~20 Å in length and 8 Å in diameter) capped by arginine lids (Fig.1a).[11] It can specifically recognize one ATP molecule by host-guest chemistry and H-bonding interactions. Inspired by its structural feature, here we have delicately designed a special biomimetic receptor-containing diblock copolymer. The artificial groups can seize ATP bioactivators by specific ligand-receptor interactions, leading to the formation of ATP/polymer complexes, which can further induce the polymer self-assembly. Moreover, owing to multiple receptors attached on the main chain, the polymer can quantitatively sense ATP amount. This offers a chance to achieve ATP-responsive cascading deformations from primary assemblies to sophisticated structures, mimicking the biological membrane remodelling (Fig. 1d).

Results and discussion

Designing synthetic ATP-receptor

To realize our goal, we target a kind of water-soluble polymer with bioinspired receptors capable of trapping ATP such that the ATP/polymer complexes can be readily formed. The ability of each independent polymer to capture the ATP is essential, as this has a profound effect not only on tuning the amounts of ligand-receptor complementary pairs but also on controlling their self-

Cite this: DOI: 10.1039/c0xx00000x

www.rsc.org/xxxxxx

ARTICLE TYPE

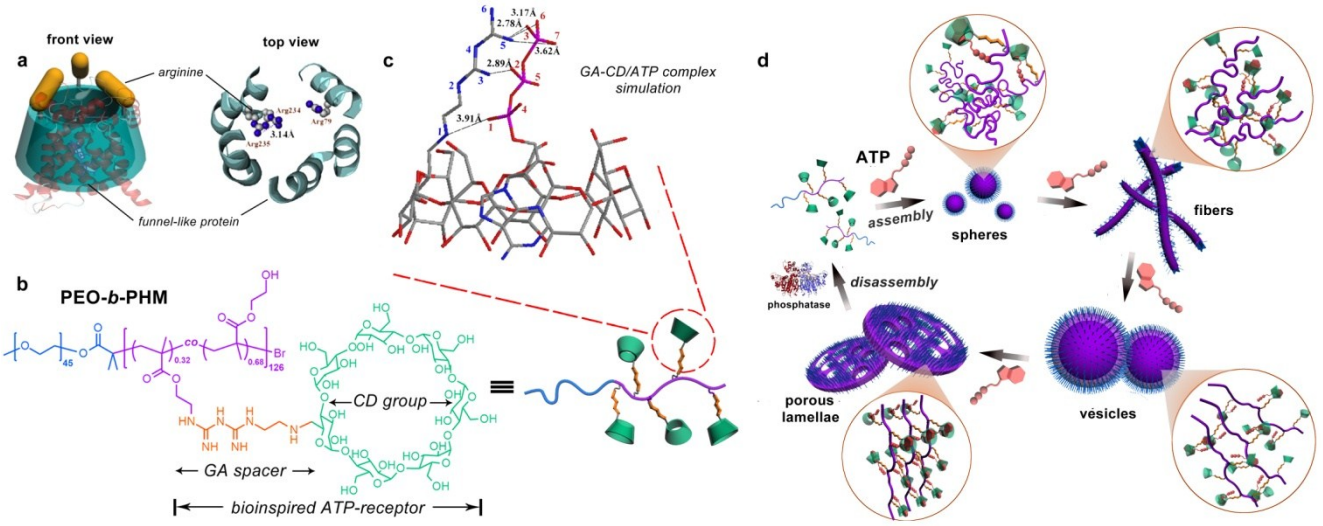

Fig. 1 (a) Natural ATP carrier protein: Front (left) and top view (right) of its funnel-like cavity and three arginine lids. (b) Chemical structure of the bioinspired receptor-containing block copolymer (PEO-*b*-PHM): its side chain has a large number of mimetic ATP-capturer composed of a biguanidine (GA) spacer and a *β*-cyclodextrin (CD) host moiety. (c) Molecular docking results of GA-CD and ATP ligand-receptor complexation (calculated by software SYSBL 7.3 methods, in which the color sticks: blue, nitrogen; grey, carbon; red, oxygen and purple, phosphorus. All hydrogen atoms are omitted for clarity). (d) ATP-triggered self-assembly and morphological transformation of these bioinspired receptor-containing block copolymers to biomimick the organellar deformations.

assembling nanostructures. We therefore synthesized a diblock copolymer, PEO_{45}-*b*-PHM_{126}, via atom transfer radical polymerization.[12] As shown in Fig. 1b, PEO is a biocompatible poly(ethylene oxide) block ($M_{n,PEO}$ = 2.0 kDa) while PHM is a functionalized host-abundant polymethacrylate block ($M_{n,PHM}$ = 66.5 kDa) in which *β*-cyclodextrin (CD) serving as macrocyclic pendants are randomly grafted onto the backbone bridged by a short biguanidine (GA) spacer (32% grafting density, each chain has ~40 pendants).[13] We expect that such a pocket-like GA-CD functionality can act as the receptor to catch ATP, because the CD moiety (7.8 Å cavity diameter) simulating the ATP carrier's funnel-like structure can bind the nucleotide species of ATP via host-guest interaction and GA spacer analogous to the arginine caps can stabilize the triphosphate species of ATP via H-bonding.

We first aimed to survey whether this bioinspired receptor could seize ATP bioactivator. Molecular docking simulation was used to study the interactions between GA-CD model compound and ATP.[14] Based on the prediction of noncovalent distances, the GA moiety theoretically form quintuple H-bonding with ATP triphosphate tail (N5—O3, 2.78 Å; N5—O6, 3.17 Å; N5—O7, 3.62 Å; N3—O2, 2.89 Å; N1—O1, 3.91 Å), and the CD moiety can envelop the nucleotide head group tightly (Fig. 1c). It implies that the GA-CD group is possible to be an efficient ATP-receptor.

Specific recognition of ATP by the polymeric receptor

According to the semiempirical simulation, our synthetic polymer can strongly bind to ATP as a result of the synergism of the H-bonding of GA/triphosphate group and the host-guest chemistry of CD/nucleotide group. To further elucidate the ATP/PEO-*b*-PHM ligand-receptor recognition, we employed ^{31}P NMR method and UV-Vis spectroscopy to respectively monitor the two classes of supramolecular interactions. In the absence of the copolymer, ATP show three phosphorus peaks at δ = -9.5 (γ-P), -10.6 (α-P), and -21.4 (β-P) ppm. Upon increasingly injecting the copolymer into ATP in the molar ratio from 1:400 to 1:10, the three initial signals are gradually weakened, accompanying with another set of broad signals of increasing intensity at δ = -7.6 (d, $^3J_{\beta,\gamma}$ = 11.4 Hz), -8.4 (d, $^3J_{\alpha,\beta}$ = 16.5 Hz) and -19.1 (dd, ^3J = 16.5, 11.4 Hz) ppm, indicating that the amount of free ATP is slowly decreasing and a new ATP complex is generated (Fig. 2a). The shifts to low field and the spin-spin splitting can be ascribed to the formation of multivalent interactions between the GA moiety and phosphate region.[15] On the other hand, UV-Vis spectra further disclose the host-guest interaction. Without the copolymer, the ATP solution displays a typical absorption of adenosine at 261 nm;[16] However, upon gradual addition of PEO-*b*-PHM, this absorption shows a double growth from 0.07 to 0.16, indicating that the adenosine species is bound to the cavity of CD to form a inclusion complex (Fig. 2b). This host-enhanced UV-absorption can be observed in other host-guest systems.[17] In addition, monitoring the proton shifts of ATP and nucleotide region by ^{1}H NMR and 2D NOSEY spectra confirms this result (Fig. S7 in ESI†). The binding stoichiometric ratio between ATP and one polymer is averagely measured to be 36 by Job's plot experiment (Fig. S8 in ESI†), being close to the copolymer grafting density (~40). It means that

Cite this: DOI: 10.1039/c0xx00000x

www.rsc.org/xxxxxx

ARTICLE TYPE

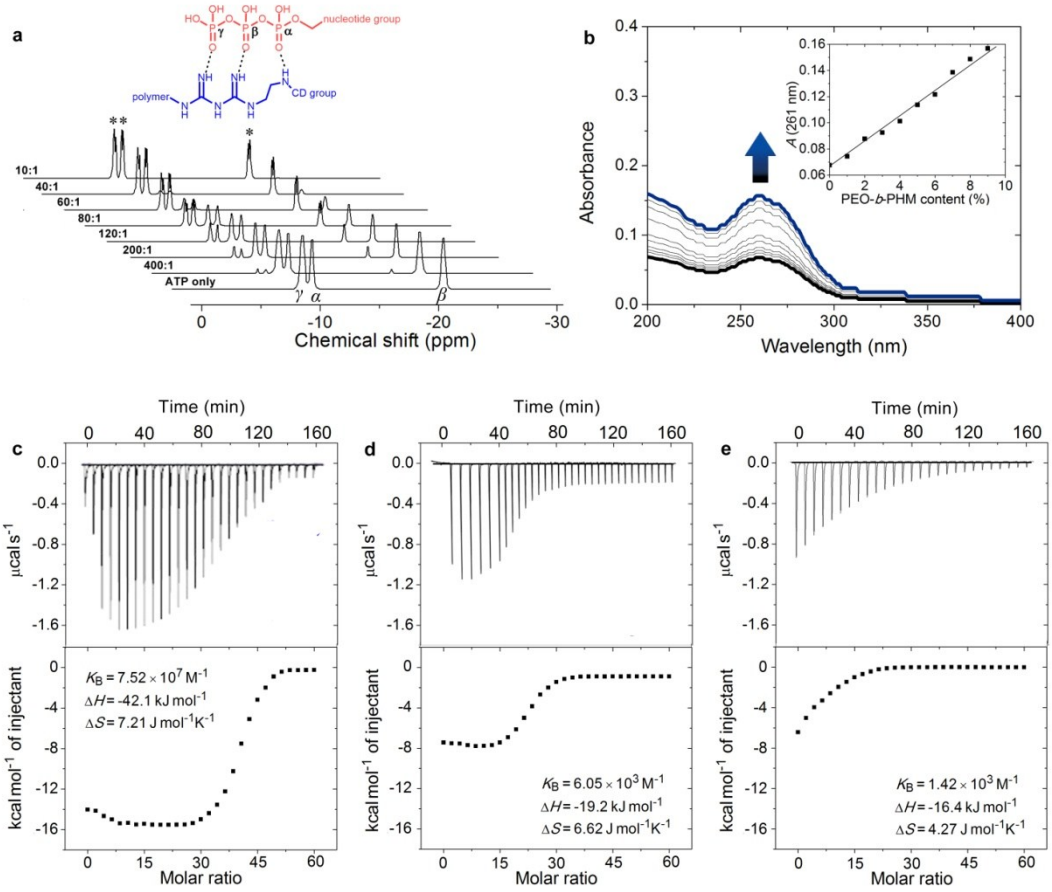

Fig. 2 ATP/polymer ligand-receptor interactions: (a) ^{31}P NMR titration of ATP (40 mM) with PEO-*b*-PHM at variable concentration ratios (D_2O). The inset shows the H-bonding interaction sites between ATP's triphosphate region and the copolymer's GA species. (b) UV-Vis absorption changes of ATP (0.1 mM) upon addition of PEO-*b*-PHM (0%~10% content). The inset gives the absorption variation (261 nm) as a function of copolymer content. (c—e) ITC results show the three ligand-receptor interactions: ATP/PEO-*b*-PHM (c), ATP/C_1 (C_1 is a copolymer counterpart without GA spacer) (d), and ATP/C_2 (C_2 is another copolymer counterpart without CD pendant) (e). Injecting 60 μM of ATP solution into 1.0 μM copolymer solution at 293 K. (All the experiments are in Tris-HCl buffer, pH = 7.20).

this polyvalent receptor can not only recognize the ATP and also respond to the amount of ATP in an almost quantitative way.

Next we aimed to understand how strong the ATP/PEO-*b*-PHM interaction is. Here we used isothermal titration calorimetry (ITC) method to resolve this problem. ITC is a quantitative technique that can directly measure biological intermolecular interactions and thermodynamic parameters.[18] Injecting ATP stock solution (60 μM) into the PEO-*b*-PHM solution (1.0 μM, Tris-HCl buffer, pH = 7.20). The binding affinity (K_B) was found to be 7.52×10^7 M^{-1}, which is the most approximate data to that of natural ATP carrier so far. The binding stoichiometry, *n*, fits to be 34.8, being consistent with the UV-Vis results. The association enthalpy and entropy are ΔH = -42.1 kJ mol^{-1} and ΔS = 7.21 J mol^{-1} K^{-1}, respectively, and the Gibbs free energy (ΔG) calculates to be -44.2 kJ mol^{-1} (Fig. 2c; Table S1 in ESI†). Since the total binding affinity arises from the H-bonding and host-guest combination, thus, we prepared two copolymer counterparts to unravel the independent contribution of the two noncovalent forces. The two counterparts, referred to C_1 and C_2, lack of the GA spacer and CD pendant, respectively (Fig. S6 in ESI†). In control experiments, the association constants and free energies are $K_B = 6.05 \times 10^3$ M^{-1} and ΔG = -21.2 kJ mol^{-1} for ATP/C_1, and $K_B = 1.42 \times 10^3$ M^{-1} and ΔG = -17.7 kJ mol^{-1} for ATP/C_2, respectively. They are both much weaker than that of ATP/PEO-*b*-PHM complex (Fig. 2d,e; Table S1 in ESI†), pointing out if the polymer only possessing individual supramolecular force is insufficient to recognize ATP biomolecules. Furthermore, on the basis of the energy terms, the independent contribution of host-guest interaction and H-bonding accounts for 48% and 40%, respectively. It is worth noting that the extra binding energy (account for 12%) results from a positive cooperative effect of GA and CD moieties (Fig. S9 in ESI†).

In the intracellular environment, there are some other biological

metabolites similar with the ATP structure. Hence we wondered whether our polymer receptor has high specificity and selectivity to ATP. As shown in Fig. 3, indeed ATP has by far the strongest binding affinity with PEO-*b*-PHM (>10^7 M^{-1}). Considering its analogues, adenosine-5'-diphosphate (ADP), due to lack of a phosphate group for forming multiple H-bonding, it is unable to form stable ligand-receptor complex, as indicated by the binding affinity decreased dramatically to $K_B = 1.9 \times 10^4$ M^{-1}. In the case of adenosine-5'-monophosphate (AMP), it cannot even associate with the polymer. Uridine-5'-triphosphate (UTP) and cytidine-5'-triphosphate (CTP) are two other interferents. Even though they have the capability to form multiple H-bonding, their binding affinities are less than ~10^3 M^{-1}. The reason is that the sizes of their nucleotide head group mismatch the CD cavity. Finally, for nicotinamide adenine dinucleotide (NADH), its bulky end-group hinders the formation of inclusion complex due to the steric effect. These results further demonstrate the high specificity to ATP of our bioinspired receptor.

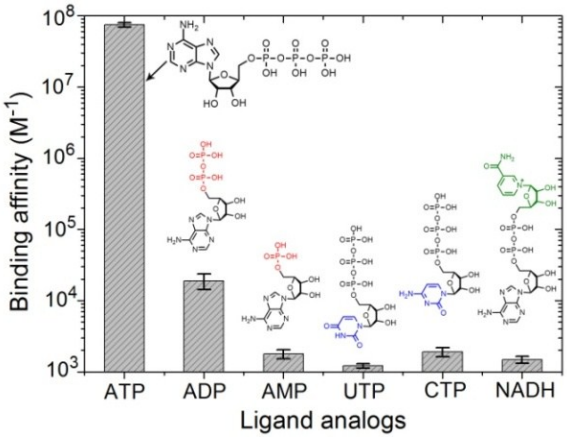

Fig. 3 The specific recognition between PEO-*b*-PHM copolymer and ATP. ATP/PEO-*b*-PHM complex shows the highest binding affinity of ~10^7 M^{-1}. Other ATP analogues (ADP, AMP, UTP, CTP and NADH) exhibit much lower binding affinity (~10^3 M^{-1}). All experiments operated by ITC (adding 60 μM of ATP into 1.0 μM copolymer solution at 293K in Tris-HCl buffer, pH = 7.20)

ATP-driven polymer self-assembly and shape transformation

Since PEO-*b*-PHM can specifically recognize ATP bioactivators, we wanted to further know investigated whether the polymer self-assembly and shape transformation can be driven by ATP. PEO-*b*-PHM is water-soluble to form homogenous and transparent solution (~0.42 mM maximum solubility). All the experiments fix the copolymer concentration at 0.20 mM (in buffer, keep pH at 7.20) and vary the ATP stimulus from 0 mM to 8 mM, which matches well with the intracellular ATP concentration (1—10 mM).[19] As we add ATP into the copolymer solution, interestingly, it becomes increasingly opaque, implying a self-assembly colloid formed (Fig. S10 in ESI†). Since the size of colloidal particle has positive correlation to solution turbidity, an ATP concentration-resolved transmittance experiment was carried out to detect the particle size change.[20] The work profile covers four fast-ascent stages and four platform stages (Fig. 4a): In the range of 0—1.6, 2.8—3.4, 4.0—4.8, and 6.4—7.0 mM of ATP, the turbidity rapidly rises 0%→18%, 20%→39%, 42%→61%, and 65%→79%, respectively, meaning that the sizes of ATP/polymer complexes undergo a stepped increase. In contrast, every plateau (S_1—S_4) between two adjacent climbing stages (1.6—2.8, 3.4—4.0, 4.8—6.4, and 7.0—8.0 mM of ATP, colourful regions in Fig. 4a) suggests that the variation of micelle dimension is negligible and, probably, corresponds to a certain stable phase. Similar results can be found in another stimuli-responsive system.[4b] Dynamic light scattering (DLS) further supports this result (Fig. 4b). By slowly exerting ATP to a given copolymer solution, in the four platform periods, the average hydrodynamic radius, R_h, shows a continuous growth from initial 5.9 nm (no ATP) to 18.5 nm (1.8 mM ATP), 57.4 nm (3.6 mM ATP), 92.8 nm (5.0 mM ATP) and 217 nm (8.0 mM ATP), respectively. Such a series of size changes reveal that the morphological differentiation of ATP/polymer complex relies on the ATP stimulation levels.

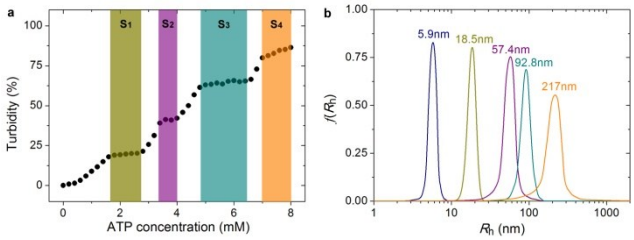

Fig. 4 (a) Turbidity changes show the four stable self-assembly phase states (S1—S4, colorful regions) and intermediate states (blank) of the PEO-*b*-PHM assemblies under different ATP levels. (b) DLS results show the size changes of the polymer assemblies in various ATP levels: navy, 0 mM; dark yellow, 1.8 mM; purple, 3.6 mM; cyan, 5.0 mM and orange, 8.0 mM (from left to right).

To visualize the deformation details in various stages, we used transmission electron microscope (TEM) to track. With the aid of a little of ATP (1.8 mM), the copolymers can self-assemble into near-monodisperse spherical micelles. They are typical corona-core structure with homogenous diameter of 31 ± 2 nm from TEM auto-statistics over 250 particles (Fig. 5a and inset; Fig. S11 in ESI†), which is in accordance with DLS results (R_h = 18.5 nm). Furthermore, the gyration radii, R_g, of these aggregates are ~14.6 nm determined by static light scattering (SLS). The shape factor, $\rho = R_g/R_h$, is used as sensitive parameter to identify the geometry of polymer aggregates.[21] In this case, the ρ value is calculated to be 0.789, corresponding to the theoretical value of solid sphere (ρ_T = 0.774, Fig. S12 in ESI†). After increasing ATP to 3.6 mM, these spheres completely vanished, instead, a great number of worm-like micelles appeared in the solution (Fig. 5b; Fig. S13 in ESI†). These nanofibers have hundreds of nanometers length and almost uniform diameter of 29 ± 3 nm. Meanwhile, the ρ value is 1.893, further ascertaining their fibrous structure (ρ_T = 1.732 for cylinders; Fig. S14 in ESI†). In view of their similar diameter to spherical micelle, they are possibly formed from the conjunction and remodelling of multiple spheres. An intermediate state with the appearance of a string of beads upon addition of 2.8 mM ATP confirms the process of linearly micellar connection (Fig. S15 in ESI†). While the ATP reaches 5.0 mM, the dominant population transformed to large vesicular nanostructures (Fig. 5c; Fig. S16 in ESI†), as confirmed by the ρ of 1.082 (ρ_T ~1 for hollow spheres; Fig. S17 in ESI†). The size of these aggregates ranges from 55

nm to 194 nm (average ~168 nm) and the wall thickness is about 11 nm. Note the tendency of the vesicles to cohere each other via the attachment of membrane. Interestingly, further improving ATP strength (7.2 mM) leads to a broad fusion among different vesicles to produce a network structure, like a large porous sponge (Fig. 5d; Fig. S18 in ESI†). In particular, the nanopore size is in line with that of the vesicles (Fig. 5e), proving the fusion mechanism. Afterwards the sponge-like objects were self-flattened, and finally adopt a kind of irregular interconnected lamellar architecture upon addition of 8.0 mM ATP (Fig. 5f; Fig. S19 in ESI†). Their average scales exceed ~500 nm and the nanopore diameter falls to 20─40 nm, indicating that these pores are compressed strongly in the flatten process. This continuous shape evolution (nanospheres→nanofibers→vesicles→porous lamellae) is in many ways reminiscent of the biological deformations.

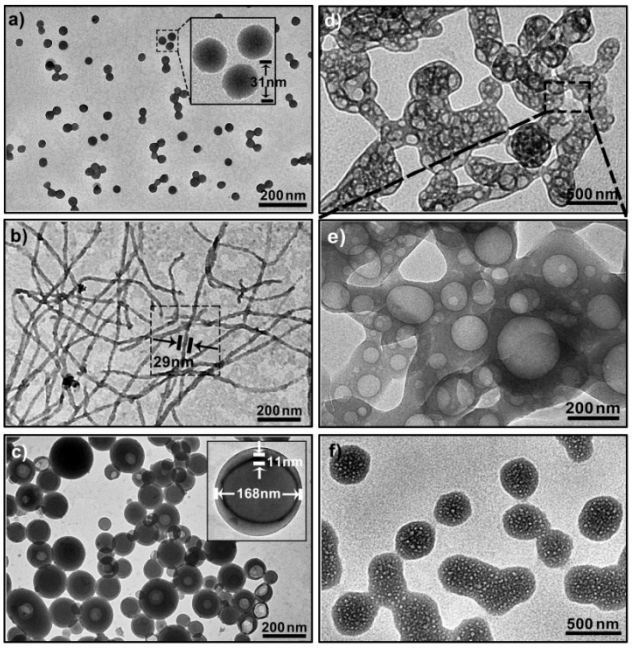

Fig. 5 TEM images of the shape transformation of the polymer assemblies under different ATP levels: a) spherical micelles upon 1.8 mM ATP, b) worm-like micelles upon 3.6 mM ATP, c) vesicles upon 5.0 mM ATP, d) fused vesicular networks upon 7.2 mM ATP and e) the magnified view for the sponge-like nanopores, f) porous interconnected lamellae upon 8.0 mM ATP. The polymer concentration is fixed at 0.20 mM in Tris-HCl buffer, pH = 7.20.

ATP-triggered deformation mechanism

This striking biomimetic polymer shape transformation depends on the block copolymer amphiphilic alterations. In the absence of ATP, PEO-*b*-PHM can be dissolved in aqueous solution. When ATP is added, they are trapped by the polymer receptors to form ATP/polymer complexes. With increasing ATP concentrations, the amount of complexed units gradually increases, resulting in a continuous molecular weight augmentation, as revealed by gel permeation chromatogram (from 68.5 kDa at 0 mM ATP to 84.1 kDa at 8.0 mM ATP; Fig. S20 in ESI†). Since the complexation segments change from hydrophilicity to hydrophobicity whereas the non-complexation portions maintain hydrophilic, the shifted hydrophilic-hydrophobic balance becomes a driving force to influence the polymer self-assembly. With the increase of ATP amount, it causes a gradual decrease of hydrophilic block volume fraction (*f*). It is known that *f* is related to the geometry of block copolymer amphiphiles. Theoretically, spheres should be formed when $f > 50\%$, worm-like micelles when $40\% < f < 50\%$, vesicles for $25\% < f < 40\%$, and other complex lamellar structures for $f < 25\%$.[22] In the case of PEO-*b*-PHM (0.20 mM), by increasing the ATP concentration, the *f* values produce a clear reduction from 77% (1.8 mM ATP) to 52% (3.6 mM ATP) to 31% (5.0 mM ATP) and finally to 12% (8.0 mM ATP), corresponding to the globular, fibrous, vesicular and lamellar structures, respectively (Table S2 in ESI†).

The specificity of ATP-driven biomimetic deformations

To be better suitable for application in the cellular environment, it is desirable that this biomimetic deformation has ATP specificity and selectivity. From the above experiments, we knew that the polymer assembly induces the solution turbidity increase. Based on this character, we surveyed the effects of some ATP analogues (Fig. S21 in ESI†). Regarding the maximum turbidity change of ATP/polymer as a reference standard, the ADP only causes 27% turbidity change even at a higher concentration (20 mM). This indicates that ADP is difficult to form available ADP/polymer complexes for further self-assembling. Moreover, because of the much weaker binding affinity to PEO-*b*-PHM, AMP, UTP, CTP and NADH have no capability to provoke the similar assembling. Direct evidence is also corroborated by TEM images (Fig. S22 in ESI†). These findings indicate that ATP is the only biosignal that can efficiently activate the polymeric shape transformation.

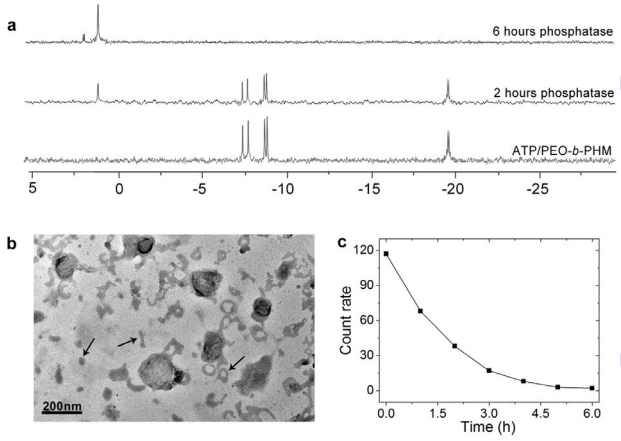

Fig. 6 (a) ^{31}P NMR spectra of ATP/PEO-*b*-PHM assemblies at various times upon addition of phosphatase. (b) TEM image of the intermediate state of the lamellar disassembly after enzyme triggered upon 2 h. (c) DLS count rate data of the ATP/PEO-b-PHM complex after treatment with phosphatase for 6 h. The polymer assemblies are kept in Tris-HCl buffer, pH = 7.20.

Enzyme-responsive disassembly

Ultimately, we expected that the ATP/polymer hybrid aggregates could be disassembled under a biological stimulus. Phosphatase is a type of enzyme that can hydrolyze ATP into free phosphate group. A small quantity of phosphatase (120 U L^{-1}), which is comparable with the average amount of phosphatase present in a

healthy adult, was injected to the ATP/polymer assemblies (lamellae). ^{31}P NMR found evidence of the enzymatic disruption of the complex. Fig. 6a shows that the complexed ATP peaks (-7.6, -8.4 and -19.1 ppm) are depressed by 45% and a new peak at 1.2 ppm ascribed to the free phosphoric acid appears upon phosphatase for 2 h. After 6 h, only phosphoric acid peak can be observed, indicating an entire dissociation of these ATP/polymer assemblies. Since the poly"complex" can respond to enzyme, we consider that this feature can be inherited to their self-assembled structure. Indeed, by treated with enzyme for 2 h, TEM discloses the intermediate state of the disassembling lamellae. As shown in Fig. 6b, it is clearly that the area of these lamellae significantly reduced from 0.5 μm down to smaller than 200 nm and a large number of nanofragments appear in the solution (arrows), which indicates a partial dissociation of these lamellar objects. Finally, these polymer aggregates completely disassembled and vanished after long-term enzyme trigger (Fig. S23 in ESI†). The count rate data from DLS also confirm that all the aggregates disappear in about 6 h (Fig. 6c).

Conclusions

In summary, we have developed a new kind of ATP-responsive block copolymer conjugated with bioinspired ATP-receptors. These synthetic macromolecules exhibit strong binding affinity ($>10^7$ M^{-1}), high specificity and selectivity to ATP bioactivator. By capturing of ATP, the polymer can form ATP/polymer hybrid complexes. One can modulate ATP stimulation levels to precisely control the self-assembly architecture with anticipant geometries, dimensionalities and shape transformable behaviors. Reversible disassembly can respond to a relative protease. We envisage that this bio-responsive polymer model will open up an avenue to take advantage of synthetic macromolecules to build smart biomimetic assemblies for imitating cellular and organellar activities.

Acknowledgements

This work was financially supported by the National Science and Engineering Research Council of Canada (NSERC) and le Fonds de recherche du Quebec: Nature et technologies (FRQNT).

Department de Chimie, Université de Sherbrooke, Sherbrooke, Québec, Canada J1K 2R1, Email: Yue.Zhao@Usherbrooke.ca

†Electronic Supplementary Information (ESI) available: See DOI: 10.1039/b000000x/

Notes and references

1 (a) G. Di Paolo and P. De Camilli, *Nature,* 2006, **443**, 651-657; (b) H. T. McMahon and J. L. Gallop, *Nature,* 2005, **438**, 590-596.

2 (a) G. K. Voeltz and W. A. Prinz, *Nat. Rev. Mol. Cell Biol.,* 2007, **8**, 258-264; (b) Y. Shibata, J. Hu and M. M. Kozlov, *Annu. Rev. Cell Dev. Biol.,* 2009, **25**, 329-354.

3 (a) J. Zimmerberg and M. M. Kozlov, *Nat. Rev. Mol. Cell Biol.,* 2006, **7**, 9-19; (b) G. K. Voeltz and T. A. Rapoport, *Cell,* 2006, **124**, 573-586.

4 (a) S. A. Meeuwissen, K. T. Kim, Y. C. Chen, D. J. Pochan and J. C. M. van Hest, *Angew. Chem. Int. Ed.,* 2011, **50**, 7070-7073; (b) Q. Yan and Y. Zhao, *Angew. Chem. Int. Ed.,* 2013, **52**, 9948-9951; (c) A. Blanazs, J. Madsen, G. Battaglia, A. J. Ryan and S. P. Armes, *J. Am. Chem. Soc.,* 2011, **133**, 16581-16587.

5 (a) S. Y. Yu, T. Azzam, I. Rouiller and A. Eisenberg, *J. Am. Chem. Soc.,* 2009, **131**, 10557-10566; (b) J. Z. Du and S. P. Armes, *J. Am. Chem. Soc.,* 2005, **127**, 12800-12801; (c) Y. Cai, K. B. Aubrecht and R. B. Grubbs, *J. Am. Chem. Soc.,* 2011, **133**, 1058-1065; (d) X. K. Liu and M. Jiang, *Angew. Chem. Int. Ed.,* 2006, **45**, 3846-3850; (e) J.-C. Eloi, D. A. Rider, G. Cambridge, G. R. Whittell, M. A. Winnik and I. Manners, *J. Am. Chem. Soc.,* 2011, **133**, 8903-8913; (f) Q. Yan, R. Zhou, C. K. Fu, H. J. Zhang, Y. W. Yin and J. Y. Yuan, *Angew. Chem. Int. Ed.,* 2011, **50**, 4923-4927; (g) A. C. Feng, C. B. Zhan, Q. Yan, B. W. Liu and J. Y. Yuan, *Chem. Commun.,* 2014, **50**, 8958-8961; (h) F. Sakai, G. S. Chen and M. Jiang, *Polym. Chem.*, 2012, **3**, 954-961.

6 (a) F. Liu and M. W. Urban, *Prog. Polym. Sci.*, 2010, **35**, 3-23; (b) D. Roy, J. N. Cambre and B. S. Sumerlin, *Prog. Polym. Sci.*, 2010, **35**, 278-301.

7 (a) L. V. Chernomordik and M. M. Kozlov, *Annu. Rev. Biochem.*, 2003, **72**, 175-207; (b) A. Kahraman, R. J. Morris, R. A. Laskowski and J. M. Thornton, *J. Mol. Biol.*, 2007, **368**, 283-301; (c) D. K. Clare, D. Vasishtan, S. Stagg, J. Quispe, G. W. Topf, A. L. Horwich and H. R. Saibil, *Cell*, 2012, **149**, 113-123; (d) Y. Z. Yin, S. Jiao, C. Lang and J. Q. Liu, *Soft Matter*, 2014, **10**, 3374-3385.

8 F. C. Ke, H. Destecroix, M. P. Crump and A. P. Davis, *Nat. Chem.*, 2012, **4**, 718-723.

9 C. S. Mahon and D. A. Fulton, *Nat. Chem.*, 2014, **6**, 665-672.

10 (a) S. Biswas, K. Kinbara, T. Niwa, H. Taguchi, N. Ishii, S. Watanabe, K. Miyata and K. Kataoka, T. Aida, *Nat. Chem.,* 2013, **5**, 613-620; (b) R. Mo, T. Y. Jiang and Z. Gu, *Angew. Chem. Int. Ed.,* 2014, **53**, 5810-5815.

11 E. Pebay-Peyroula, C. Dahout-Gonzalez, R. Kahn, V. Trézéquet, G. J. Lauquin and G. Brandolin, *Nature,* 2003, **426**, 39-44.

12 K. Matyjaszewski and J. H. Xia, *Chem. Rev.,* 2001, **101**, 2921-2990.

13 (a) O. Peters and H. Ritter, *Angew. Chem. Int. Ed.*, 2013, **52**, 8961-8963; (b) O. Jazkewitsch, A. Mondrzyk, R. Staffel and H. Ritter, *Macromolecules*, 2011, **44**, 1365-1371; (c) A. Harada, R. Kobayashi, Y. Takashima, A. Hashidzume and H. Yamaguchi, *Nat. Chem.*, 2011, **3**, 34-37; (d) H. Yamaguchi, Y. Kobayashi, R. Kobayashi, Y. Takashima, A. Hashidzume and A. Harada, *Nat. Commun.*, 2012, **3**, 603.

14 D. B. Kitchen, H. Decorez and J. R. Furr, *Nat. Rev. Drug Discov.*, 2004, **3**, 935-949.

15 D. Q. Yuan, A. Izuka, M. Fukudome, M. V. Rekharsky, Y. Inoue and K. Fujita, *Tetrahedron Lett.,* 2007, **48**, 3479-3483.

16 R. M. Bock and N.-S. Ling, *Arch. Biochem. Biophys.,* 1956, **62**, 253-264.

17 (a) Y. P. Wang, N. Ma, Z. Q. Wang and X. Zhang, *Angew. Chem. Int. Ed.*, 2007, **46**, 2823-2826; (b) Q. Yan, Y. Xin, R. Zhou, Y. W. Yin and J. Y. Yuan, *Chem. Commun.*, 2011, **47**, 9594-9596.

18 S. Leavitt and E. Freire, *Curr. Opin. Struc. Biol.,* 2001, **11**, 560-566.

19 M. Leist, B. Single, A. F. Castoldi, S. Kuhnle and P. Nicotera, *J. Exp. Med.,* 1997, **185**, 1481-1486.

20 D. H. Melik and H. S. Folger, *Colloid Interf. Sci.*, 1983, **92**, 161-180.

21 G. Zhang and C. Wu, *Phys. Rev. Lett.,* 2001, **86**, 822-825.

22 B. M. Discher, Y. Y. Won, D. S. Ege, J. C. Lee, F. S. Bates, D. E. Discher and D. A. Hammer, *Science,* 1999, **284**, 1143-1146.